Indian Journal of Chemistry
Vol. 63, April 2024, pp. 358-366
DOI: 10.56042/ijc.v63i4.6822

Magnetic cellulose composite for cyanide adsorption from water

Anita Shekhawat*[a], Ravin Jugade[a], Vaishnavi Gomase[a], Shashikant Kahu[a], Sadanand Pandey[b] & Saravanan Dhandayutham[c]

[a] Department of Chemistry, R. T. M. Nagpur University, Nagpur 440 033, India

[b] Department of Chemistry, College of Natural Science, Yeungnam University, 280 Daehak-Ro, Gyeongsan, Gyeongbuk, 38541, Republic of Korea

[c] Department of Chemistry, National College, Tiruchirappalli 620 001, India

E-mail: annushekh22@gmail.com

Received 20 November 2023; accepted (revised) 22 March 2024

In this study, aluminium doped mesoporous magnetic cellulose (AMMC) has been synthesized by co-precipitation method. The prepared adsorbent has been utilized for the adsorption of cyanide. The characteristic changes in the structural specifics of the adsorbent have been analyzed by techniques like FTIR, SEM, EDX, XRD, BET, VSM and TGA-DTA. The magnetic behavior of the material contributes in easy handling during its utilization in the adsorption process. Adsorption studies have been carried out at *p*H 8.0 with 0.1 g of adsorbent through batch adsorption process. Isotherm studies reveal that adsorption of cyanide on AMMC proceeds through monolayer phenomenon with adsorption capacity of 34.46 mg/g. Adsorption kinetics of the process have been explained through pseudo second order model. Adsorption of cyanide shows spontaneity with enthalpy driven process. Effect of interfering anions on adsorption have also been studied. Large quantities of cyanide containing water samples can be treated with AMMC through column adsorption method. Regeneration of the material and the number of adsorption-desorption cycles have proven that the adsorption of cyanide through AMMC is an ecofriendly process.

Keywords: Mesoporous, Magnetic cellulose, Biopolymer, Cyanide, Optimization, Regeneration

Cyanide is a toxicant present in water bodies as a result of discharge from various industries like electroplating, mining, pesticides, fumigants, plastics, *etc*.[1] Cyanide worsening of water has adversely affected aquatic life as well as flora and fauna. Excess of cyanide in water causes several problems including nausea, digestive and lung problem, acute poisoning and may also lead to anexia. It has direct interaction with iron in metalloenzymes which is associated with cellular respiration[2]. According to WHO, the permissible limit of cyanide in water is 0.05 g mL^{-1} whereas US Environmental Protection Agency (USEPA) has set the limit of 200 and 50 ppb for drinking[3]. Considering the disastrous impact of cyanide, the water should be treated before discharging it directly into the environment. There are various advanced technologies were processed for the removal of cyanide like precipitation, coagulation, ion exchange, reverse osmosis, membrane filtration and adsorption[4]. Out of all these methodologies adsorption considered as more effective and environmentally benign. Various adsorbents like metal oxides, organic polymers, biopolymers used for the removal of cyanide.

Metal oxides acts as a potent adsorbent having large surface area, a greater number of active sites, thermal stability and easy recovery. In spite of all these properties this metal oxides show dissolution in acidic conditions. To overcome this, various researchers fabricate composite materials with polymers. Biopolymers like cellulose, chitosan, chitin are the well- known for the incorporation of metal oxides of Fe, Ti, Al, Zr, Mg and their bimetallic oxide[5]. Cellulose is β-D-glucose units linked together and is important component of cell wall of plants, algae and oomycetes. Cellulose is hydrophilic, acts as a sorbent and having hydroxyl functionality for facile modifications. Extensive inter and intramolecular hydrogen bonding in cellulose provides mechanical strength. Bio composites involving metal oxides having excellent affinity for the adsorptive removal of anionic moieties is well known[6,7].

In present work, the cyanide removal studies were performed using batch adsorption method utilizing AMMC. Parameters for adsorption were optimized, various isotherm and kinetic models were examined for understanding the adsorption process. The material possesses excellent adsorption capacity

towards cyanide as compared to that of native cellulose.

Materials and Method

Chemicals and reagents

Analytical grade reagents were used for the adsorption of cyanide. All the aqueous solutions are prepared in double distilled water. 1000 mg L^{-1} cyanide stock solution was prepared from sodium cyanide (Merck, India). Microcrystalline cellulose was purchased from SRL Chemie Ltd. India. Spectrophotometric method has been utilized for the determination of cyanide in water[8].

Preparation of AMMC

A gel solution of cellulose was prepared in a mixture of NaOH /Urea /Thiourea/Water[9]. At the same time, a solution was prepared having 0.1M $FeCl_3$, 0.05M $FeSO_4$ and 0.1M $AlCl_3$ in distilled water was prepared with continuous stirring at 60°C. The metallic mixture acts as a coagulation bath for extrusion of cellulose. Cellulose solution was added drop wise into coagulation bath of metallic solution resulting in dark magnetic meso-composite. While washing an external magnet placed below the coagulation bath for quick setting of magnetic particles and supernatant was removed through decantation. The precipitate was washed with same procedure with deionized water till negative test of chloride was obtained. The AMMC composite was dried at 60°C in a vacuum oven.

Characterization of adsorbent

FT-IR characterization of AMMC was performed by Bruker*Alpha*E spectrometer. Righaku-Miniflex 300 X-ray diffractometer was used for recording XRD spectra. TESCAN VEGA 3 SBH scanning electron microscope with X- ray analyzer Oxford INCA Energy 250 EDS System was used for SEM-EDS analysis. Thermal stability of AMMC was studied using Shimadzu DTG-60. Surface area and pore-volume of AMMC has been studied through Quantachrome Nova 2200e.

Batch adsorption study

0.1g of AMMC equilibrated with 5-200 mg L^{-1} for 60 minutes at *p*H 7.0 in a stoppered conical flask for batch adsorption studies. The amount of cyanide adsorbed on AMMC q_e in mg g^{-1} and percentage removal at equilibrium can be calculated by using mathematical equations 1 respectively

$$q_e = \frac{C_0 - C_e}{W} \times V \quad \text{...(1)}$$

where C_0 is the initial cyanide concentration and C_e is the cyanide concentration at equilibrium in mg L^{-1}, V and W is the volume of Cyanide solution in liter and weight of AMMC in grams respectively. Three replicates of batch adsorption experiments were performed to obtain authentic results.

Results and Discussion

Characterization of adsorbent

Fig. 1a shows FTIR spectrum of pure cellulose having a broad peak at 3331 cm^{-1} which is assigned to O–H stretching. A strong peak of C-O-C skeletal vibration is observed at 1043 cm^{-1} and a peak at 1318 cm^{-1} could be attributed to CH_2 wagging. In AMMC (Fig. 1b), the peak at 699 cm^{-1} and 566 cm^{-1} are assigned to Fe-O and Al-O respectively[10], whereas the values 3394 cm^{-1} and 1645 cm^{-1} are for –OH stretching and –OH bending respectively. The regenerated cellulose composite through metallic solution clearly shows that aluminium and iron hydroxides were integrated into the cellulose. Due to the formation of inter and intra molecular hydrogen bonds, the cellulose exhibits a crystalline nature with two diffracted peaks at 2θ = 16.52° and 22.61°[11] (Fig. 1b). The XRD pattern of AMMC shows the diffraction peaks at 2θ values of 30.15, 35.52, 37.18, 43.17, 53.5, 57.11, 62.7, 89.89, and 89.98. The magnetite exists in two different phases Fe^{2+} and Fe^{3+} ($FeO.Fe_2O_3$) and shows a peak at 32.31 (crystallographic pdf No. 01-083-0112) which is attributed to FeO which is a less stable phase. The Fe^{2+} present in octahedral sites is replaced by aluminum[12]. The incorporation of aluminium and iron oxides in cellulose was confirmed by the values which matched with JCPDS 76-1157[13]. The value calculated from Debye-Scherrer equation shows the average crystal size was 74.92nm. The SEM micrographs shows surface morphology of the material and gives an idea of structural changes as a result of modification of cellulose. Fig. 1c shows fibrous surface of cellulose whereas on impregnation with iron and aluminium oxides shows granular imprints which provides active available sites for adsorption. The EDX spectrum of cellulose shows only peaks of carbon and oxygen and AMMC displays the peaks of Fe and Al along with oxygen and carbon peaks of cellulose.

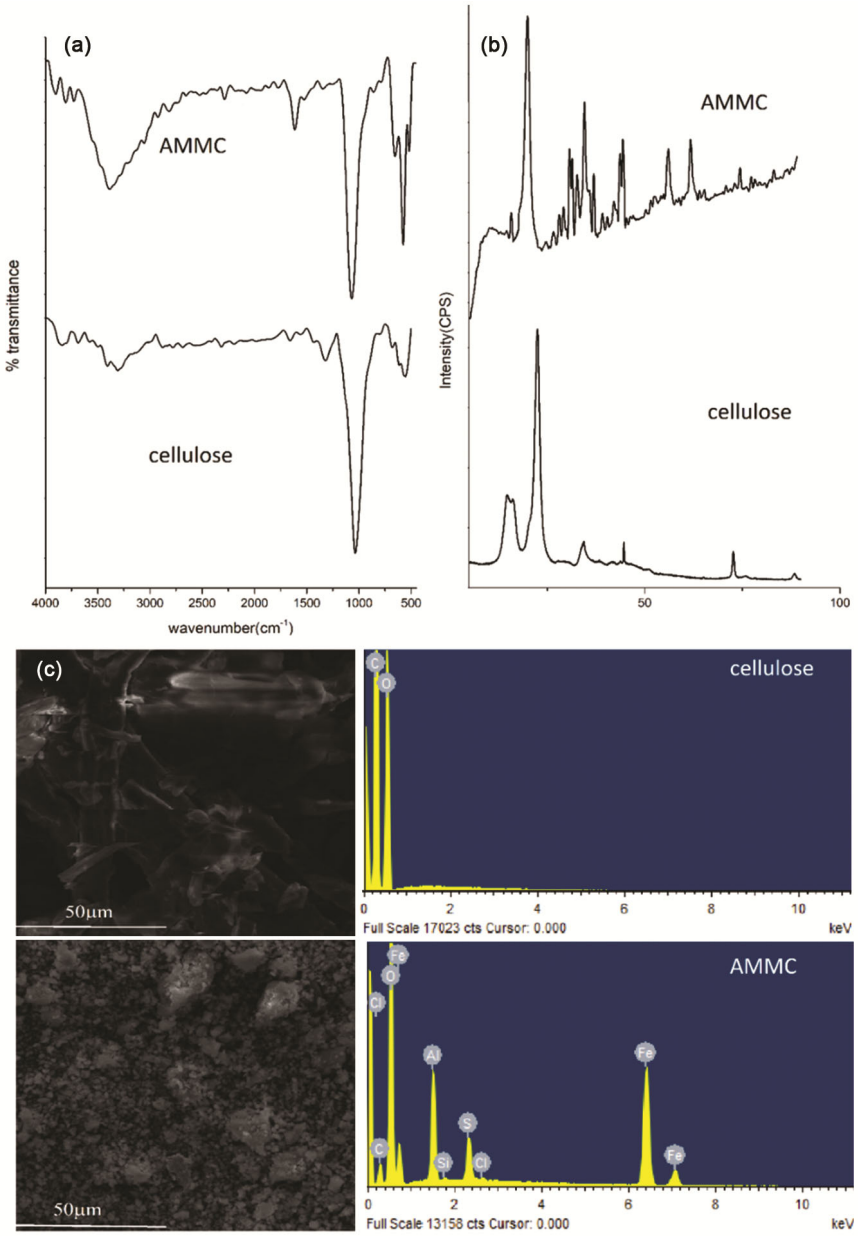

Fig. 1 — (a) FTIR, (b) XRD and (c) SEM-EDX

The thermogram of cellulose (Fig. 2a) shows one step degradation. Cellulose shows a sharp decrease in % weight in the range of 250-350°C. An endothermic peak is observed in DTA in the range of 50-100°C which is due to loss of moisture and a second endotherm is observed in the range 300-400°C which is ascribed to the breaking of polysaccharide chain[14]. Similarly, AMMC shows degradation between 350-400°C and has enhanced thermal stability as compared to cellulose. The % weight loss remarkably reduced from 80% of cellulose to 18% AMMC and is stable in entire temperature range which depicts excellent thermal stability attributed to the casting of aluminium and iron oxides into the cellulose matrix. DTA (Fig. 2b) of adsorbent shows loss of water molecule at 100°C and a sharp exotherm around 370°C indicating breakdown of Al and Fe linkages with the cellulose chain and destruction of polymeric chain of cellulose.

The native cellulose has a surface area 16.63 m^2/g with pore volume of 0.018 cm^3/g. The surface area was increased to 97.38 m^2/g with pore volume of 0.179 cm^3/g in AMMC as aluminium doped magnetite iron is incorporated into the matrix of cellulose. The average pore diameter of 7.386 nm reveals the mesoporous nature

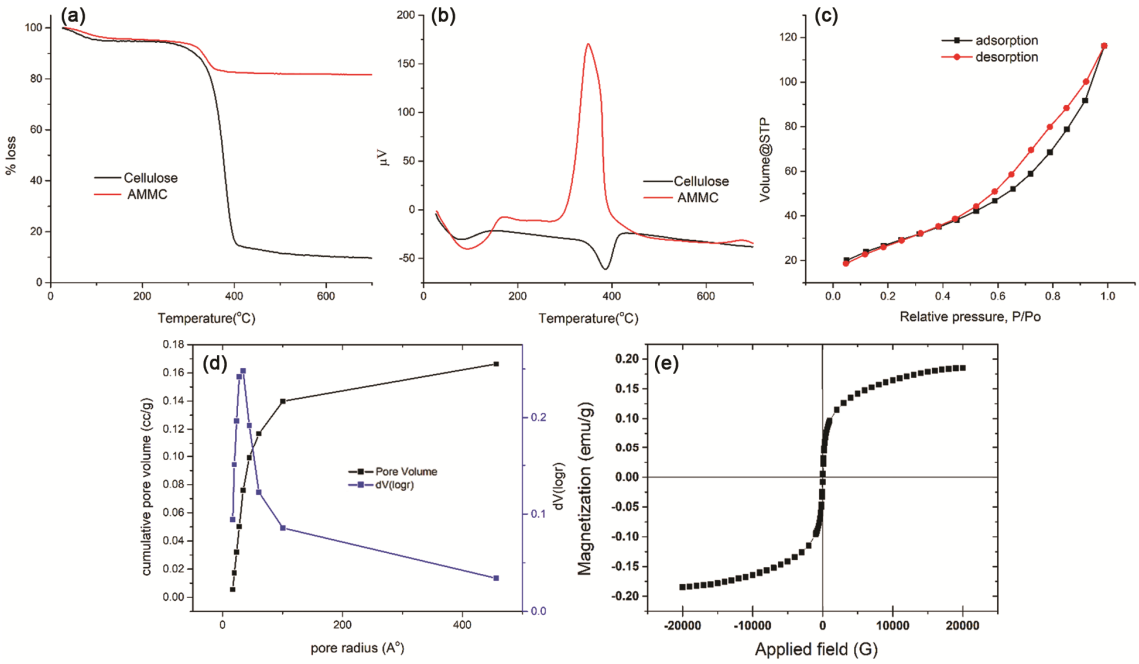

Fig. 2 — (a) TGA of cellulose and AMMC, (b) DTA of cellulose and AMMC, (c) adsorption –desorption curve of AMMC, (d) pore size distribution of AMMC and (e) magnetic -hysteresis (M-H) loop at RT of AMMC

of AMMC which matches with the standard values given by IUPAC[15]. Fig. 2c shows a hysteresis loop which is of type IV isotherm based on adsorption-desorption curve and Fig. 2d gives the pore size distribution which indicates the adsorbent has a complex structure with mesopores[16]. The complex nature of surface can be observed in SEM micrograph. The lower limit of the hysteresis is decided by the shapes of mesopores. Ultimately, the increased surface area with pore volume contributes for high adsorption capacity of AMMC. Changes in the surface area of cellulose confirms the formation of the modified cellulose adsorbent.

Magnetic property of mesocomposite AMMC was determined by magnetic -hysteresis (M-H) loop at RT. Fig. 2e shown that obtained hysteresis obtained were due to ferromagnetic behavior of the mesocomposite particles of moderate saturation magnetization with no coercivities. The saturation magnetization value was found to be 0.1475 emu/g from M-H loops. Since, the material is having cellulose as a non-magnetic material as a result of that the value of saturation magnetization is low. Due to the sensitive response towards the magnet, the handling of AMMC throughout the experiment becomes easier.

Parameters optimization

The cyanide solution of varying *p*H from 6-10 were stirred with AMMC to analyze the effect of *p*H on the adsorption. It was observed that initially with increase in *p*H from 6-8 the adsorption of cyanide increases whereas from 8-10 *p*H it starts decreasing. The maximum adsorption of cyanide on AMMC was observed at *p*H 8 (Fig. 3a). AMMC point of zero charge is 8.6 (Fig. 3e). At *p*H 8, the surface of AMMC is positively charged and HCN dissociates into CN^- ions which attributes for increase in adsorption capacity of the material. Therefore, the optimum *p*H value for the adsorption is 8.0.

The amount of AMMC was varied from 0.025g to 0.4g to investigate the effect of adsorbent dose on adsorption process. It is obvious with increase in successive adsorbent dose, the adsorption percentage increases (Fig. 3b). When the dose of AMMC reaches to 0.1 g, the % removal was found to be 88%. After that increase in dose does not shows the remarkable change in the % adsorption due to less amount of cyanide ions in the equilibrating solution as compared to adsorption sites. The amount of cyanide adsorbed remains constant with increase in AMMC dose, as a result the equilibrium adsorption capacity goes on decreasing. Thus, for further adsorption studies 0.1 g of AMMC was utilized.

Similarly, the effect of contact time and cyanide concentration was studied. It was found that with increase in time the percentage removal and adsorption capacity is also increasing and reaches to equilibrium in 90 min (Fig. 3c). At this duration, no adsorption sites are available for further interaction of

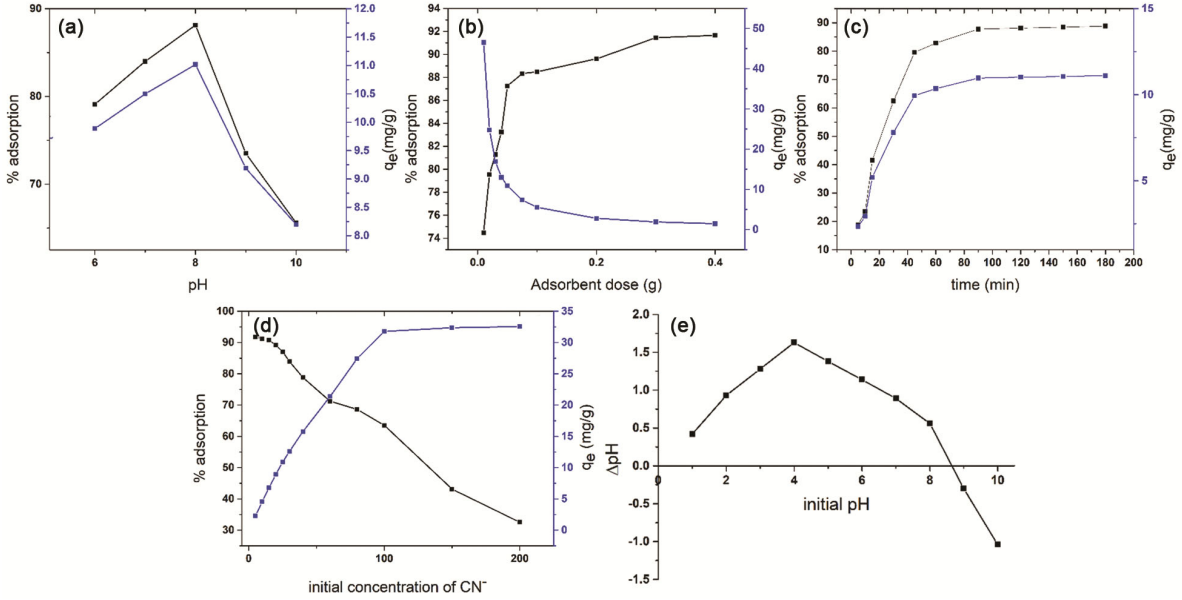

Fig. 3 — Optimized parameters (a) *p*H, (b) AMMC dose, (c) time, (d) initial concentration and (e) *p*H point of zero charge

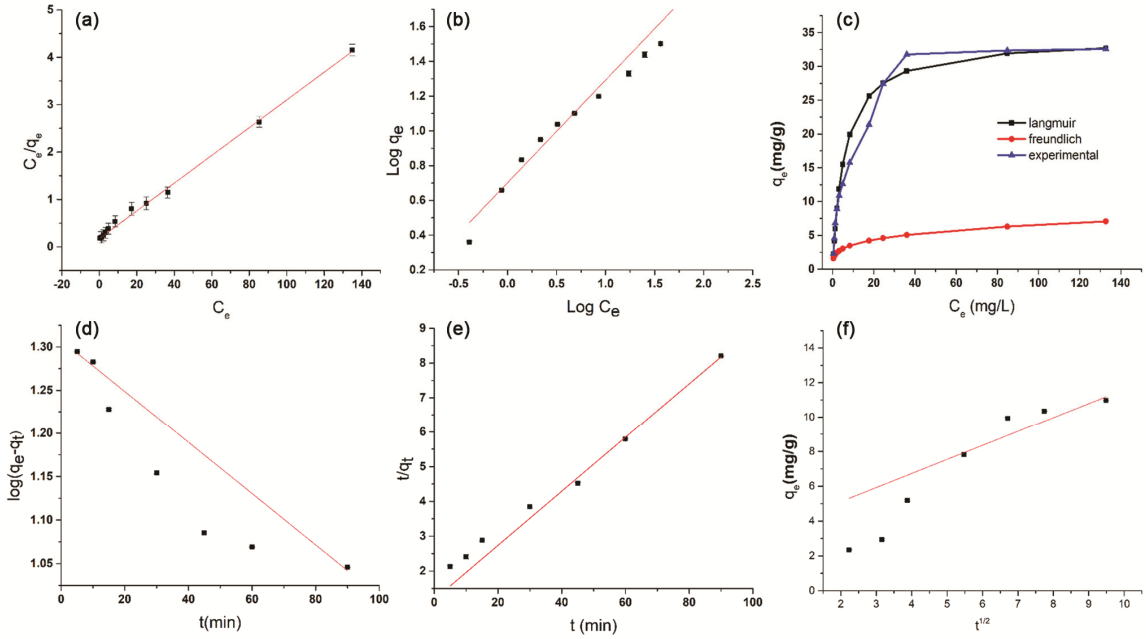

Fig. 4 — (a) Langmuir isotherm, (b) Freundlich isotherm, (c) comparison of isotherm with experimental data, (d) pseudo first order (e) pseudo second order and (f) intra-particle diffusion

cyanide. Therefore, 90 min were optimized for adsorption studies.

At 5 mg/L of cyanide, the percentage removal was found to be more than 92% (Fig. 3d) due to ample number of adsorption sites availability. With increase in concentration of cyanide ions, the adsorption sites were occupied successively and reached to saturation as a result percentage removal goes on decreasing and adsorption capacity goes on increasing. Hence, 5 mg/L fixed for the adsorption studies.

Isotherm models

In Langmuir isotherm model[17], q_0 was found to be 34.16 mg/g which refers to the maximum adsorption capacity through monolayer adsorption whereas b represents the Langmuir constant related to energy and calculated through the values of slope and intercept of plot C_e/q_e *versus* C_e (Fig. 4a). Separation factor R_L value found to be less than 1 which favors the effective interaction between AMMC and cyanide

Table 1 — (a) Adsorption isotherms parameters and (b) Kinetic models parameters

Sr. No.	Models	Parameters	Value
	Adsorption isotherms		
1	Langmuir $C_e/q_e = 1/q_0 b + C_e/q_0$ $R_L = \frac{1}{1+bC_0}$	q_0 (mg g^{-1})	34.16
		b(L mg^{-1})	0.168
		R_L	0.192
		r^2	0.997
		AIC	29.52
		AIC $_{corrected}$	41.52
2	Freundlich $\log q_e = \log K_F + \frac{1}{n} \log C_e$	K_F ($mg^{1-1/n} g^{-1} L^{-1}$)	5.029
		n	1.692
		r^2	0.960
		AIC	79.18
		AIC $_{corrected}$	89.18
	Kinetic models		
1	Pseudo-first-order kinetics $\log(q_e - q_t) = \log q_e - \frac{k_1 t}{2.303}$	k_1 (min^{-1})	0.006
		r^2	0.986
		AIC	31.13
2	Pseudo-second -order kinetics $\frac{t}{q_t} = \frac{1}{k_2 q_e^2} + \frac{t}{q_e}$	k_2 (g $mg^{-1} min^{-1}$)	0.005
		r^2	0.994
		AIC	8.46
3	Intraparticle diffusion $q_t = k_{int}.t^{1/2} + C$	K_{int} (mg/g/$min^{1/2}$)	0.810
		r^2	0.717

(Table 1). log q_e *vs*. log C_e plot for Freundlich adsorption isotherm gives Freundlich adsorption capacity 'k_F' and adsorption intensity 'n' [18] (Fig. 4b). The value 1.692 of n favors cyanide interaction with AMMC. The value of correlation coefficient and AIC [19] for Langmuir isotherm shows that it is best fitted model to explain interaction of cyanide with AMMC. The same result was obtained through comparison q_e calculated from isotherm with experimental q_e.

Adsorption Kinetics

Pseudo first order (PFO), Pseudo second order (PSO) and Weber-Morris kinetic models were studied at optimized parameters to understand the adsorption kinetics. The time interval varied from 5 to 90 min for calculating various kinetic parameters. The respective equations for kinetic models and parameters values were mentioned in Table 1.

The rate constants for PFO and PSO were calculated from the plot of log ($q_e - q_t$) against t (Fig. 4d) and plot of log t/ q_t against t (Fig. 4e) respectively. PSO found to be most suitable isotherm from the value of regression coefficient for PSO, lower AIC value and q_e experimental value was closer to the q_e calculated.

Weber-Morris model was studied in order to determine the rate limiting step. Weber -Morris model traces the plot of $t^{1/2}$ *vs*. q_t (Fig. 4e.). The non-zero intercept concludes that adsorption intra-particle diffusion is not only the rate determining step and the process goes through boundary layer adsorption and reaches to equilibrium.

Thermodynamics of adsorbent

The thermodynamic parameters were calculated at varying temperature to know the feasibility of the adsorption process. Equations 5 and 6 were used to calculate ΔG, and ΔS

$$\Delta G = -RT\ln K \quad \ldots(2)$$

$$\ln K = \frac{\Delta S^0}{R} - \frac{\Delta H^0}{RT} \quad \ldots(3)$$

whereas R is the gas constant (8.314 J/mol/K). ΔH (kJ/mol) and ΔS (kJ/mol/K) values were obtained from the slope and intercept of the plot of ln K against 1/T (Fig. 5a). Spontaneous and exothermic behavior of the adsorption process was confirmed by the negative values for free energy change and enthalpy change (Table 2). The decrease in concentration of cyanide ions in the solution phase through adsorption

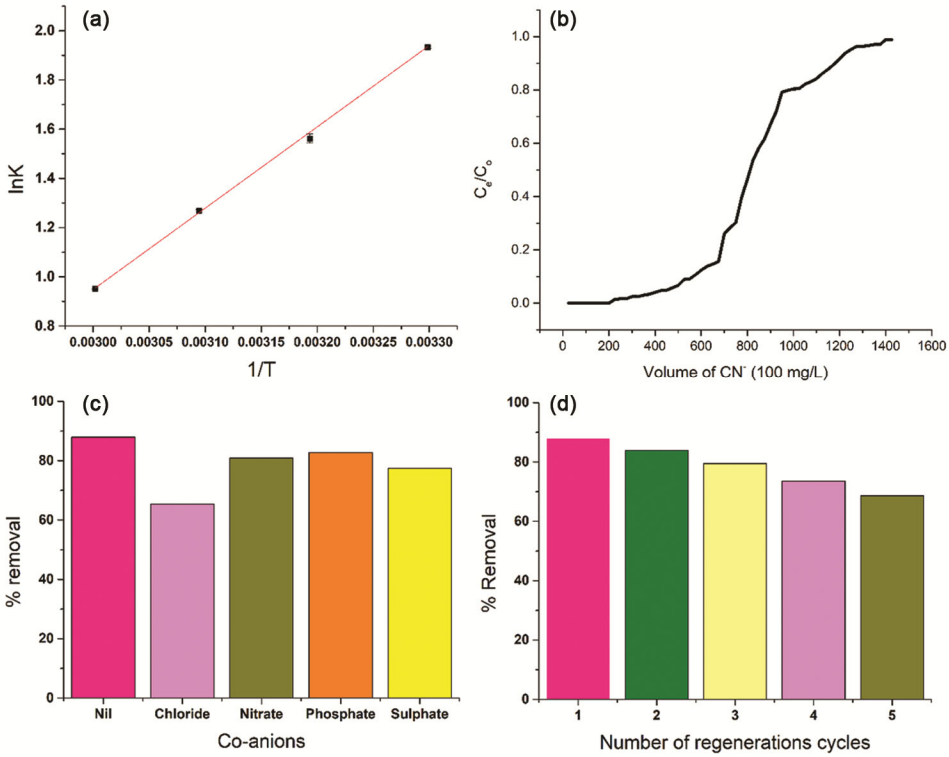

Fig. 5 — (a) van't Hoff plot, (b) Breakthrough curve, (c) Effect of co-anions and (d) Regeneration cycles

Table 2 — Thermodynamic parameters of adsorption

Temperature (K)	ΔG(kJ/mol)	ΔH(kJ/mol)	ΔS(kJ/mol/K)
303.15	–4.870	–27.476	–0.074
313.15	–4.066		
323.15	–3.408		
333.15	–2.637		

on the surface of AMMC, decrease in randomness of cyanide ions on the surface of AMMC resulting into negative entropy change.

Effect of co-anions

In case of real samples, presences of other ions may interfere in the adsorption process leads to decrease in the adsorption capacity due to competition for the active sites. For this 1mM concentration of co-anions like SO_4^{2-}, Cl^-, NO_3^-, CO_3^{2-}, PO_4^{3-} were studied along with same concentration of cyanide ions one by one through batch adsorption process (Fig. 5c). It was observed that chloride ions interfering more in the adsorption process.

Regeneration of AMMC

The material is sustainable and environmentally friendly such predictions were possible when it can be regenerated after utilization. For this, cyanide desorption studies were carried out with reagents such as sodium chloride, sodium nitrate, sodium sulphate and sodium carbonate. It was found that cyanide can be desorbed effectively with 5% (v/v) sodium nitrate solution. The regenerated AMMC was tested for ten adsorption-desorption cycles and it was found that for first five cycles there is minor change in adsorption efficiency (Fig. 5d). However, the adsorption efficiency successively decreases to 62% for the tenth cycle.

Cyanide Sorption Mechanism

The increased adsorption of cyanide on AMMC can be explained by means of molecular binding iron and aluminium oxides to the surface of cellulose containing hydroxyl groups as well as glycosidic linkages of cellulose biopolymer. The metal ion present on AMMC adsorbent can interacts with the cyanide ions in two ways. It has protonated surface groups which forms strong electrostatic attraction with cyanide ions and can exchange hydroxide ions with cyanide ions. However, the porous structure reinforces the adsorption of cyanide anion on the AMMC through diffusion also.

Table 3 — Column study of field sample

Inlet concentration	Breakthrough Volume (mL)	Exhaustion Volume (mL)	Breakthrough capacity (mgg^{-1})	Exhaustion capacity($mg\ g^{-1}$)	Degree of column utilization (%)
100	575	1200	115	240	47.91

Table 4 — Application of adsorbents to synthetic effluent

Synthetic effluent	Concentration of ions ($mg\ L^{-1}$)	CN^- conc. ($mg\ L^{-1}$)	% Removal
A	Cl^- (950), SO_4^{2-} (80), NO_3^- (300), PO_4^{3-} (400), F^- (50), Zn^{2+} (100), Fe^{2+} (300), Fe^{3+} (100), Ni^{2+} (50), Mg^{2+} (200), Cu^{2+}(50)	25	68.63 ± 2.00
	Cl^- (605), SO_4^{2-} (1600), NO_3^- (150), PO_4^{3-} (200), F^- (25), Zn^{2+} (200), Fe^{2+} (300), Fe^{3+} (200), Ni^{2+} (100), Mg^{2+} (200), Cu^{2+}(100)	25	71.36 ± 2.00

Column Study

About 0.5 g sorbent was packed in glass column of 30 cm length with 1 cm diameter. The cyanide was passed through the column at 5 mL/min flow rate. The cyanide concentration was measured in the eluent collected after every 10 min. Leaching of iron and aluminium were also tested in the eluent but the results were negative. From Fig. 5b and the results obtained in Table 3, it was observed that this material can be used for larger volumes of samples and can give better results with more optimized conditions.

Applicability on synthetic effluents

Two synthetic effluents A and B, similar to real samples were prepared having two different compositions to test the applicability of the AMMC. The results are shown in Table 4.

Comparison with reported materials

The effectiveness of the material was checked by comparison of adsorption capacities of various reported adsorbents for cyanide (Table 5).

Sustainability

The sustainability parameters for AMMC were analysed for synthesis and adsorption process are shown in Table 6.

These parameters indicate the approaches towards the environmental concerns during the formation of material through chemical reactions and utilization through adsorption process. The results are depicted in Table 5. The raw materials used for the material synthesis were nontoxic. All the solutions were prepared in aqueous medium, which can be reused and recycled. The alkaline medium was used to dissolve cellulose which helps in co-precipitation of acidic solution of iron and aluminium salts. Raw materials used for synthesis were easily available and affordable. Mass intensity was found to be

Table 5 — Comparison with other adsorbents

Adsorbent	Adsorption capacity ($mg\ g^{-1}$)	Reference No.
Raw and modified coke	1.28	20
Calcinated eggshells	3.27	21
Copper impregnated coconut shell activated carbon	5.30	22
Cetyl trimethylammonium bromide activated red mud	19.50	23
Ch-PLK	24.69	24
Prunus amygdalus (almond) shell	32.05	25
AMMC	34.16	Present study

Table 6 — Sustainability parameters

Parameter	Value
Mass intensity	$2.45\ kg\ kg^{-1}$
Water intensity	$67.31\ kg\ kg^{-1}$
Reaction mass efficiency	49.01%
E- Factor	0.017

$2.45\ kg\ kg^{-1}$. This value can be reduced to unity by minimizing loss of product during filtration and washing. Since large amount water was used for washing and for adsorption process, the water intensity was found to be $67.31\ kg\ kg^{-1}$. This spent water can be stored and recycled. Reaction mass efficiency 49.01% was obtained. 1 g of adsorbent purifies approximately 1.2 L of water sample having CN^- ($100\ mg\ g^{-1}$) in a single process and this figure can be increased by regeneration of the material.

Conclusion

Cellulose availability in environment has been used for bioremediation by superficial modification. Cellulose forms crosslinked gel solution with urea and thiourea along with sodium hydroxide. On addition of acidic solution of metals into the cellulose gel, cellulose gets regenerated along with Al doped magnetite in its core. Negative results of leaching of iron and aluminium indicates that the composite is stable. It possesses higher surface area and is mesoporous in behavior. AMMC possessed higher

adsorption capacity for cyanide adsorption due to electrostatic force of attraction, ion exchange phenomena and diffusion. The sorption of cyanide on AMMC followed Langmuir isotherm. Column studies indicated that AMMC could be used as an effective adsorbent for cyanide for larger sample volumes also. The regeneration and sustainable studies of AMMC reveals that the material can be used effectively for the cyanide adsorption in a greener way.

Acknowledgments

All the authors acknowledge RTM Nagpur University for providing necessary research facilities. Dr. Anita Shekhawat is thankful to CSIR-HRDG, New Delhi for providing Research Associateship [09/128(0099)/2020-EMR-I].

References

1 Monser L & Adhoum N, *Sep. Purif. Technol*, 26 (2002) 137.
2 Chena S C & Liu J K, *FEMS Microbiol. Lett*, 175 (1999) 37.
3 Young C A & Jordan T S, *Cyanide Remediation: Current And Past Technologies*, 26.
4 Dash R R, Gaur A & Balomajumder C, *J. Hazard. Mater*, 163 (2009) 1.
5 Pinto R J B, Neves M C, Neto C P, Trindade T, Pinto R J B, Neves, M C, Neto C P, & Trindade T. *IntechOpen* (2012) ISBN 978-953-51-0762-0.
6 Anjum A, Adsorption Technology for Removal of Toxic Pollutants. In *Sustainable Heavy Metal Remediation: Volume 2: Case studies*; Rene, E.R., Sahinkaya, E., Lewis, A., Lens, P.N.L., Eds.; Environmental Chemistry for a Sustainable World; Springer International Publishing: Cham, 2017; pp. 25–80 ISBN 978-3-319-61146-4.
7 Wang S, Liu Y, Yang A, Zhu Q, Sun H, Sun P, Yao B, Zang Y, Du X & Dong L, *Polymers*, 14 (2022)1107.
8 Lambert J L, Ramasamy Jothi & Paukstelis J V, *Anal Chem*, 47 (1975) 916.
9 Yu X, Kang D, Hu Y, Tong S, Ge M, Cao C & Song W. *RSC Adv*, 4 (2014) 31362.
10 Xu C, Li J, He F, Cui Y, Huang C, Jin H & Hou S. *RSC Adv*, 6 (2016) 97376.
11 Du L, Wang J, Zhang Y, Qi C, Wolcott M & Yu Z, *Nanomaterials*,7 (2017) 51.
12 Thirumoorthy K, Gokulakrishnan B, Satishkumar G, Landau M V, Man M W C & Oliviero E, *Catal Sci Technol*, 11 (2021) 7368.
13 Chaudhary M, Rawat S, Jain N, Bhatnagar A & Maiti A, *Carbohydr Polym*, 216 (2019) 140.
14 Leal G F, Ramos L A, Barrett D H, Curvelo A A S & Rodella C B, *Thermochim. Acta*, 616 (2015) 9.
15 Thommes M, Kaneko K, Neimark AV, Olivier J P, Rodriguez-Reinoso F, Rouquerol J & Sing K S W. *Pure Appl. Chem*, 87 (2015) 1051.
16 Sing K S W & Williams R T, *Adsorpt Sci Technol*, 22 (2004) 773.
17 Langmuir I, *J Am Chem Soc*, 40 (1918) 1361.
18 Freundlich H, *Z Für Phys Chem*, *57U* (1907) 385.
19 Akpa O M & Unuabonah E I, *Desalination*, 272 (2011) 20.
20 Hattab Z, Filali N, Mazouz R Guerfi, Rebbani N, Nafa A & Kheriaf S, *Desalination Water Treat*, 57 (2016) 3522.
21 Eletta O A A, Ajayi O A, Ogunleye O O & Akpan I C, *J Environ Chem Eng*, 4 (2016)1367.
22 Singh N & Balomajumder C. *Water Process Eng*, 9 (2016) 233.
23 Deihimi N, Irannajad M & Rezai B, *Environ Earth Sci*, 78 (2019)187.
24 Gomase V, Jugade R, Doondani P, Deshmukh S, Saravanan D & Pandey S, *Int J Biol Macromol*, 223 (2022) 636.
25 Dwivedi N, Balomajumder C & Mondal P, *Water Resour Ind*, 15 (2016) 28.